In situ monitoring and characterization of SiC interface formed in carbon films grown by pulsed laser deposition*

E. C. Samano, G. Soto,[a] J. Valenzuela, and L. Cota
Laboratorio de Ensenada, Instituto de Física, UNAM, Apartado Postal 2681, 22800 Ensenada, B.C., México

(Received 7 November 1995; accepted 2 May 1997)

Very thin, smooth, and uniform carbon films have been produced by ablating a pyrolytic graphite target using an ultraviolet pulsed excimer laser at fixed energy in an ultrahigh vacuum system. The films were deposited on a Si (111) surface at room temperature. The deposition process is investigated *in situ* by analyzing the time evolution of spectra obtained by Auger electron, x-ray photoelectron, and electron energy loss spectroscopies at different stages of the film growth. A relationship of the atomic concentration of Si and C with the number of laser pulses and film thickness is obtained from the spectra. A SiC interface with a thickness between one and two monolayers is observed to be formed during the very first deposition pulses. The study of this SiC buffer layer is particularly relevant when a carbon film is used as a hard coating, where strong adhesion of the film to the substrate is required. © *1997 American Vacuum Society.* [S0734-2101(97)00405-3]

I. INTRODUCTION

Pulsed laser deposition (PLD) is a novel technique to grow thin films of conducting, semiconducting, and dielectric materials based on the photoevaporation of a solid target.[1,2] The laser beam ablates the target and a plume is produced, which is composed by free radicals with a few tens of eV in kinetic energy. The presence of very energetic species in the ablation plume leads to a high instantaneous deposition rate per pulse, 10^4-10^6 Å/s. Hence, PLD is suitable for small-scale production of multilayered heterostructures, and homogeneous amorphous,[3] crystalline,[4] layer-by-layer,[5] and stoichiometric[6] thin films of very controlled thickness. Among the heterostructures currently being investigated are those systems belonging to the group IV/group IV. In particular, the study of the interface of C/Si is interesting because there is a large difference between the lattice constant of the materials involved, a 52% lattice mismatch for diamond structure, compared to systems like Si/Ge, a 4% mismatch.

The study of carbon deposition is also one of the most active research areas in thin films because they may produce hard noncrystalline carbon films, generically named diamondlike carbon (DLC).[7–9] The properties of DLC films are exceptional: good optical, chemical, and mechanical properties; regarding the last property, it has high hardness to wear resistance and shear stress. Traditionally, diamond films have been grown by chemical vapor deposition (CVD) using a catalyst, like hydrogen, at a gas pressure between 1 and 500 Torr and substrate temperature in the 600–1300 °C range. The various characterization techniques have verified the presence of both the sp^2 and sp^3 bonding in DLC films, but there is a lack of long range order.[9] CVD is widely used to grow DLC films because solid targets of carbon are difficult to evaporate by most techniques.

Nowadays, the growth of carbon films by PLD is an area of intense research because homogeneous films with high adhesion at low substrate temperature without catalysts in an ultrahigh vacuum (UHV) system can be produced. In recent studies, Collins *et al.*[10] and Pappas *et al.*[11] have grown hydrogen-free carbon films by PLD. They have found that the microstructure in the films is sensitively dependent on the impingement flux and average kinetic energy of the ablated species, mostly in the 50–200 eV energy range. The films showed a high sp^3/sp^2 ratio, meaning that charged and very energetic atoms are critical precursors of sp^3 bonding.

Therefore, the quality and bonding configuration of a carbon thin film depend on both: the kinetic process which controls the chemical structure and the interface formed during the early growth stages. This study can be carried out in a very precise manner by means of analytical techniques in the same system where the deposition process is performed. Unfortunately, there are few reports in the literature about *in situ* growth and characterization of carbon films. For instance, Belton *et al.*[12,13] have studied the nucleation and growth of diamond films by CVD and they performed *in situ* characterization by means of x-ray photoelectron spectroscopy (XPS) and electron energy loss spectroscopy (EELS) spectra. During the early stages of the deposition process, they observed the formation of a SiC interface but no quantification about the film or interface was reported. Martín-Gago *et al.*[14,15] have grown DLC films by PLD on clean Si (100) at room temperature. The film growth evolution was analyzed *ex situ* using Auger electron spectroscopy (AES) and ion scattering spectroscopy (ISS), and did not observe the existence of a SiC interface. After a postdeposition heating treatment of the DLC films at 950 °C for 10 min, they actually noticed the formation of SiC due to the interdiffusion of C and Si.

*No proof corrections received from author prior to publication.

[a]Also at Programa de Posgrado en Física de Materiales, Centro de Investigación Científica y de Educación Superior de Ensenada, 22800 Ensenada, B.C., México.

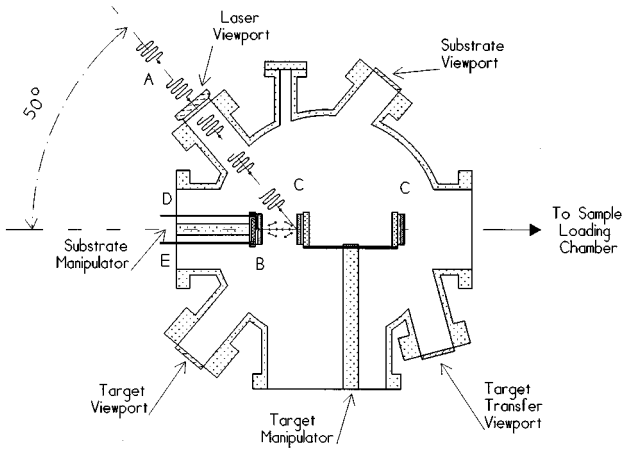

FIG. 1. Cross-sectional view of deposition chamber. (A) Pulsed laser beam, (B) substrate, (C) targets, (D) thermocouple, and (E) resistive heater.

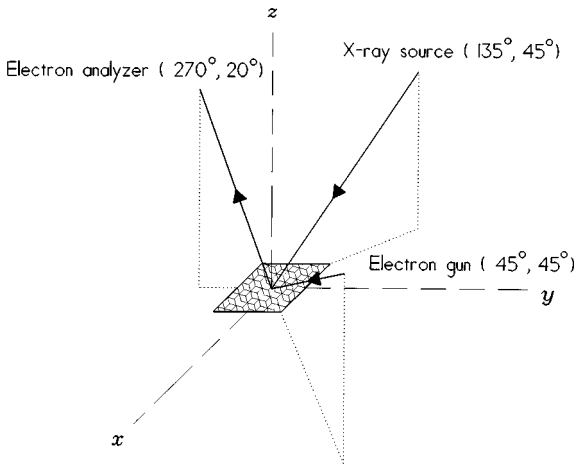

FIG. 2. Sketch showing the direction of each apparatus in the analysis chamber in terms of the azimuthal, ϕ, and polar, θ, angles as (ϕ,θ) pairs.

The present work reports the identification and quantification of the different species involved in the growth of carbon films by PLD using *in situ* surface spectroscopies. The main goal is the study of the film–substrate interface. This is achieved by ablating a high purity pyrolytic graphite target using an ultraviolet (UV) pulsed excimer laser in an UHV environment, and observing the initial stages of the deposition process. The ablated species are adsorbed on a clean Si (111) surface kept at room temperature. The experiment is momentarily interrupted at selected growth times to qualitatively and quantitatively analyze the film evolution using AES, XPS, and EELS. The possible existence of a SiC interface is also investigated. The details of the experimental setup, procedure, and results can be found in Secs. II and III, respectively. The quantitative analysis is described in Sec. IV. Finally, the analytical and experimental results, and the main conclusions of this work are discussed in Sec. V.

II. EXPERIMENTAL SETUP

The carbon films growth and characterization are performed *in situ* in a laser ablation system Riber© LDM-32. The system basically consists of three stainless steel UHV vacuum chambers; sample rapid loading, deposition, and analysis. Each chamber is isolated and independently pumped by ion and Ti sublimation pumps with a pumping speed of a few hundred liters per second in the pressure range of a typical experimental run. A couple of transfer rods allow *in vacuo* interchamber linear motion of the target and substrate, only one at a time, during the different steps of the overlayer processing.

The loading chamber is provided with a viewport access door with an O-ring vacuum seal, hence the base pressure is in the high 10^{-9} Torr, to mount up to two samples, disks as big as 2 in. in diameter, on a storage manipulator with heaters.

The films are grown in the deposition chamber, base pressure $\lesssim 2\times10^{-10}$ Torr. The chamber comprises a heated substrate station and a rapid switching targets manipulator as the main parts, as shown in Fig. 1. The substrate station includes motorized continuous rotation for uniform deposition and motion along its axial direction. The motorized targets manipulator has a four-way cross sample holder which can store up to four targets. It allows x-y-z translations, being the z direction along the surface normal, resulting in a substrate–target adjustable separation from 2 to 4 in. The output of a pulsed KrF excimer laser, Lambda Physik© LEXtra 200, enters through the laser viewport, aiming the target at an angle of 50° off normal. The nominal laser wavelength is 248 nm with a pulse length of 34 ns. The pulse repetition rate can be changed from 0.5 to 30 Hz and the operating energy is in the 50–700 mJ range.

The analysis chamber, base pressure $\gtrsim 2\times10^{-10}$ Torr, consists of a CAMECA MAC 3©, XPS-AES, system. As many as two samples are held in place on a heated manipulator. The electron gun, the x-ray source and the electron analyzer point to a specimen along the directions depicted in Fig. 2. An Ar ion gun is also available in the chamber for sputter cleaning purpose.

III. EXPERIMENTAL PROCEDURE AND RESULTS

The experiment is based on the photoevaporation of a commercially available pyrolytic graphite target, a $2\times1/16$ in. disk with 99.999% purity. The substrate is a 2×0.010 in. Si (111) wafer. The substrate was cleaned by the following procedure before being introduced into the loading chamber. It is firstly dipped in a 1:1 volume solution of H_2O_2 and H_2SO_4 for 15 min, then plunged in distilled water for 5 min, later washed in HF for 25 s, and finally rinsed in distilled water. The target is packed under Ar by the manufacturer and no cleaning procedure is believed to be necessary.

Prior to any deposition, both the substrate and target surfaces were analyzed. The Si (111) surface is previously heated at 600 °C for 3 h and annealed at 850 °C for 1.5 h[16,17] to remove the ''native'' oxide, typical in all silicon surfaces, and recover its long-range crystallinity. Afterwards, a survey

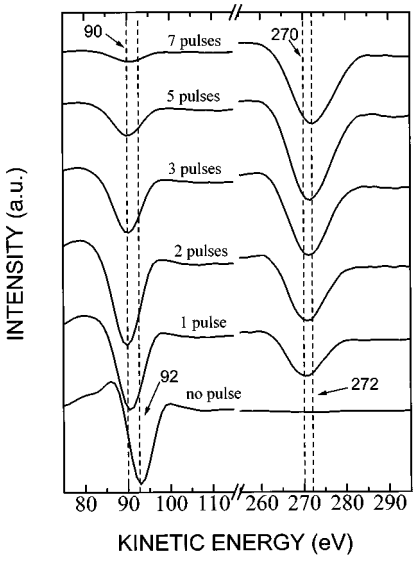

FIG. 3. AES spectra of the different stages of carbon film growth on Si (111) at room temperature. The no pulse curve corresponds to the clean Si (111) substrate.

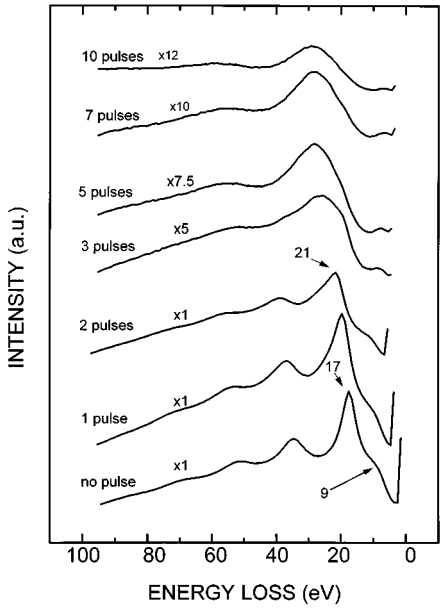

FIG. 4. EELS spectra of the different stages of carbon film growth on Si (111) at room temperature. The no pulse curve corresponds to the clean Si (111) substrate.

scan and high resolution scans using XPS of the C($1s$), Si($2p$), and O($1s$) regions are obtained for both specimens. The x-ray source of the CAMECA system produces two kinds of x-ray lines with energies $h\nu(\mathrm{Mg}\ K\alpha) = 1253.6$ eV and $h\nu(\mathrm{Al}\ K\alpha) = 1486.6$ eV. The XPS scans are done using photons with an energy of $h\nu(\mathrm{Al}\ K\alpha) = 1486.6$ eV. Similarly, the Auger transitions are investigated in the 50–600 eV energy range using an electron gun with a 3 keV incident energy. Plasmon losses are studied by EELS using an electron beam with a 1 keV incident energy. This technique is particularly sensitive in distinguishing several carbon phases and carbides present in the film.[18] The resolution in energy of the spectra is found to be 3 eV for AES, 2.3 eV for EELS, measured from the full width at half-maximum (FWHM) value of the elastic peak, and 1.2 eV for XPS, evaluated from the FWHM value of C($1s$) peak.

No C or oxides on the clean substrate and a negligible amount of oxides on the clean target were found as determined by AES and XPS scans in Fig. 3. The EELS spectrum of the clean substrate shows a well defined peak at 17 eV with harmonics at 34 and 52 eV, as shown in Fig. 4 (no pulse curve). The relative intensity of the harmonic peaks with respect to the main peak is a clear indication that the Si (111) surface is highly crystalline.[13] The target EELS spectrum shows strong peaks at 28 and 55 eV, characteristic of pyrolytic graphite,[13,19] as seen in Fig. 5(a). This spectrum is used as a reference to determine the carbon phase of the films grown in this application.

The substrate and target were then transferred to the deposition chamber to start the carbon film growth. The target surface is uniformly swept by the laser beam using the motorized manipulator. The ablated carbon species are deposited on the clean Si surface at room temperature, which is kept at a target–substrate distance of ~2 in. The laser is operated at a fixed pulse repetition rate of 1 Hz and the beam is focused to an area of ~0.1 cm^2. Before the actual depositions, the growth of carbon overlayers was attempted in the 2 to 5 J/cm^2 fluence range. The threshold fluence for detecting carbon deposition from AES and XPS spectra was found to be 2 J/cm^2, but this signal was almost imperceptible because the peaks were comparable to the background noise. The best results were found at a fixed fluence of 5 J/cm^2, and

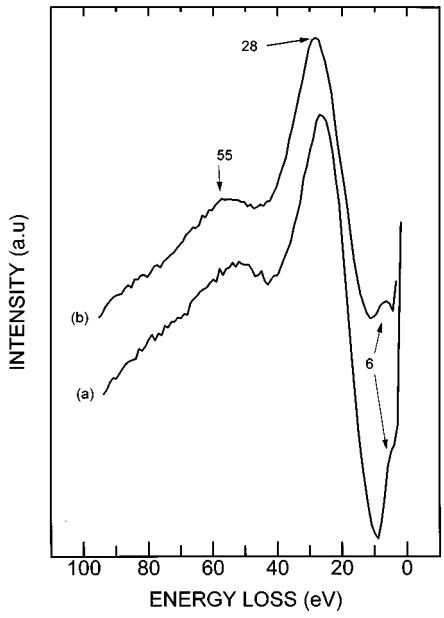

FIG. 5. Comparison of EELS spectra of the (a) pyrolytic graphite target and (b) carbon film after ten laser pulses of deposition.

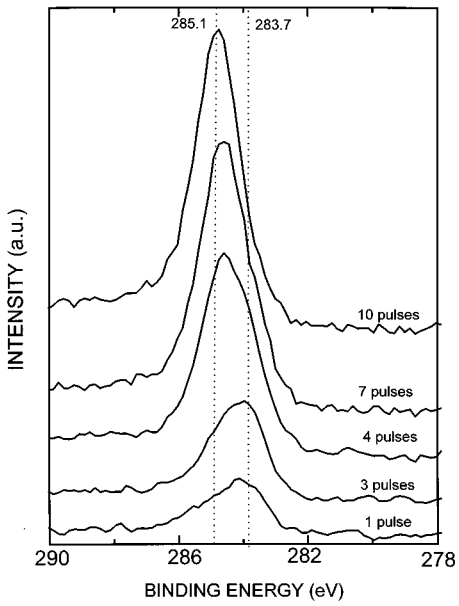

FIG. 6. XPS spectra in the C (1*s*) region of the different stages of carbon film growth on Si (111) at room temperature.

those are the ones reported in this work. The maximum chamber pressure is 2×10^{-9} Torr during deposition.

To have a better understanding of the film growth evolution, a time-dependent characterization of the surface is obtained. The deposition of carbon overlayers on Si (111) is temporarily interrupted at selected time intervals, number of laser pulses, to transfer the resulting film to the analysis chamber to be characterized by AES, XPS, and EELS. As soon as the film is analyzed, it is returned to the deposition chamber where the overlayer processing is continued. Figures 3, 4, and 6 show the AES, EELS, and XPS spectra, respectively, of the different film growth stages or ''snapshots'' of a typical deposition process. Figure 5 shows the main peaks due to plasmon losses obtained by EELS for the graphite target and a film after ten laser pulses of deposition. It is important to mention that the EELS spectra do not change in shape for depositions beyond ten pulses.

IV. QUANTITATIVE ANALYSIS

The thickness of a film can be estimated by measuring the signal intensity of a certain element in a matrix containing a homogeneous binary solid. As is well known, the measured atomic concentration, X_{Si} of Si and X_C of C in the film are directly proportional to the signal intensity I_{Si} of Si and I_C of C, respectively, taken from the AES and XPS spectra for several number of pulses:[20]

$$X_{\mathrm{Si}}(N)=\frac{I_{\mathrm{Si}}(N)/S_{\mathrm{Si}}}{[I_{\mathrm{Si}}(N)/S_{\mathrm{Si}}]+[I_{\mathrm{C}}(N)/S_{\mathrm{C}}]}, \tag{1}$$

$$X_{\mathrm{C}}(N)=\frac{I_{\mathrm{C}}(N)/S_{\mathrm{C}}}{[I_{\mathrm{Si}}(N)/S_{\mathrm{Si}}]+[I_{\mathrm{C}}(N)/S_{\mathrm{C}}]}. \tag{2}$$

In Eqs. (1) and (2), S_{Si} is the instrumental sensitivity factor for the Si $(2p)$ peak or *LVV* transition of the clean substrate for XPS or AES, respectively, and S_{C} is the sensitivity factor for the C $(1s)$ peak or *KLL* transition of the target for XPS or AES, respectively, N is the number of laser pulses.

As a first approach, the quantification of AES and XPS spectra can be done using simple analytical expressions based on the assumptions that the effects of elastic electron scattering is negligible, and the surface is a thin layer consisting of tens of monolayers or less. Theoretically, the intensity I^*_{Si} of the substrate, referred to the measured intensity $I_{\mathrm{Si},0}$ of the clean Si (111) surface, covered by a C overlayer of thickness d is given by[20]

$$I^*_{\mathrm{Si}}(d)=I_{\mathrm{Si},0}\exp\left(-\frac{d}{\lambda_{\mathrm{SC}}(E_{\mathrm{Si}})\cos\alpha}\right), \tag{3}$$

and the intensity I^*_{C} of the C overlayer, referred to the measured intensity $I_{\mathrm{C},0}$ of the graphite target, is correspondingly given by

$$I^*_{\mathrm{C}}(d)=I_{\mathrm{C},0}\left[1-\exp\left(-\frac{d}{\lambda_{\mathrm{CC}}(E_{\mathrm{C}})\cos\alpha}\right)\right]. \tag{4}$$

In Eqs. (3) and (4), α is the polar angle between the electron analyzer direction and the surface normal, given as $\alpha=20°$ in Fig. 2, λ_{SC} and λ_{CC} are the inelastic mean free paths of electrons ejected with energies E_{Si} by a Si atom and E_{C} by a C atom, respectively, moving into the C overlayer. The E_{Si} and E_{C} values depend on the binding energy of a core level electron or Auger transition electron energy of the type of spectra involved in the calculation, either XPS or AES.

The expressions for the estimated atomic concentration content of Si and C, X^*_{Si} and X^*_{C}, in the film can be obtained using Eqs. (3) and (4):

$$X^*_{\mathrm{Si}}(d)=\frac{I_{\mathrm{Si},0}\exp\left(-\frac{d}{\lambda_{\mathrm{SC}}(E_{\mathrm{Si}})\cos\alpha}\right)}{I_{\mathrm{Si},0}\exp\left(-\frac{d}{\lambda_{\mathrm{SC}}(E_{\mathrm{Si}})\cos\alpha}\right)+I_{\mathrm{C},0}\left[1-\exp\left(-\frac{d}{\lambda_{\mathrm{CC}}(E_{\mathrm{C}})\cos\alpha}\right)\right]}, \tag{5}$$

$$X^*_{\mathrm{C}}(d)=\frac{I_{\mathrm{C},0}\left[1-\exp\left(-\frac{d}{\lambda_{\mathrm{CC}}(E_{\mathrm{C}})\cos\alpha}\right)\right]}{I_{\mathrm{Si},0}\exp\left(-\frac{d}{\lambda_{\mathrm{SC}}(E_{\mathrm{Si}})\cos\alpha}\right)+I_{\mathrm{C},0}\left[1-\exp\left(-\frac{d}{\lambda_{\mathrm{CC}}(E_{\mathrm{C}})\cos\alpha}\right)\right]}. \tag{6}$$

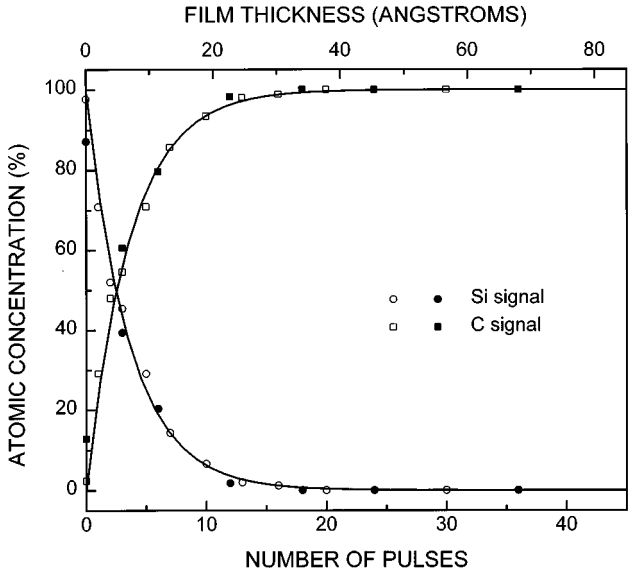

FIG. 7. Measurements of the overlayer atomic concentration of each specie, shown as symbols, for two different films grown by PLD as a function of the film thickness and number of laser pulses using the AES data. The solid lines correspond to the analytical expressions given in Sec. IV.

The X_{Si} and X_C values are found by Eqs. (1) and (2) for two different depositions as a function of the number of laser pulses. These experimental data are obtained from the AES and XPS data and displayed as symbols in Figs. 7 and 8, respectively. The X^*_{Si} and X^*_C values are calculated by Eqs. (5) and (6) as functions of the film thickness, these calculations are depicted as curves in Figs. 7 and 8. The values of λ_{SC} and λ_{CC} have been estimated following the procedure described by Powell *et al.*[21–23]

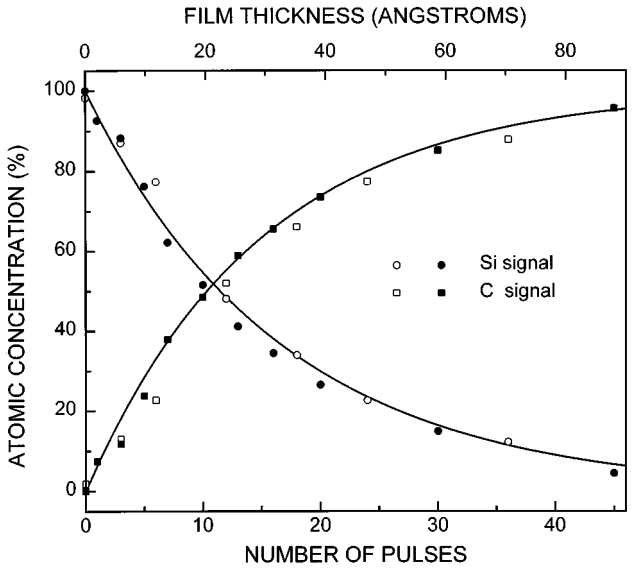

FIG. 8. Measurements of the overlayer atomic concentration of each specie, shown as symbols, for two different films grown by PLD as a function of the film thickness and number of laser pulses using the XPS data. The solid lines correspond to the analytical expressions given in Sec. IV.

As observed from Figs. 7 and 8, the number of laser pulses, N, and film thickness, d, are assumed to depend on each other. This is a reasonable consideration when the film is very thin. A relationship between these two parameters can be attained by solving

$$X_{Si}(N=1)=X^*_{Si}(d). \tag{7}$$

Substituting Eqs. (1) and (5) into Eq. (7), and using the signal intensities for one pulse taken from the AES and XPS spectra, $d(N=1)=2.04$ Å is obtained. Actually, the same value was also found by means of

$$X_C(N=1)=X^*_C(d). \tag{8}$$

Then d and N are postulated to be linearly related, at least for very thin film films, by

$$d=(2.04\ \text{Å})N. \tag{9}$$

V. DISCUSSION AND CONCLUSIONS

The first stages of a hydrogen-free carbon film growth prepared by PLD in an UHV system using different spectroscopies *in situ* has been investigated. The AES spectra change in shape and intensity as material is deposited on the substrate surface, as shown in Fig. 3. The characteristic sharp peak at 92 eV associated to Si-*LVV* Auger transition of the clean substrate, no pulse curve in Fig. 3, has changed to a peak at 90 eV after one laser pulse of deposition. The sharp peak at 85 eV has also turned into a broad and less pronounced peak after the first laser pulse of deposition. Simultaneously, the one pulse curve in Fig. 3 also shows that a new signal develops at 270 eV. According to the literature, these features are associated to the chemical binding of the materials involved in the deposition to form SiC.[24,25] As the number of laser pulses is increased, these two peaks shift in energy and change in shape and intensity. The flat shoulder at 270 eV smoothly transforms to the well known C-*KLL* Auger peak at 272 eV when the number of pulses goes from one to seven, as shown in Fig. 3. As expected, a very small signal of Si-*LVV* Auger transition is still observed after seven pulses in Fig. 3. A fully developed C-*KLL* Auger peak corresponding to the highly oriented pyrolytic graphite (HOPG) type[15,19] is identified after 30 pulses, but not shown.

Similarly, the EELS and XPS spectra change in shape and intensity as the carbon species are deposited on the substrate surface, as shown in Figs. 4 and 6, respectively. Before the carbon deposition, the EELS spectrum of the clean substrate shows a shoulder at a plasmon energy loss of 9 eV and a main peak at 17 eV with several harmonics, as observed in Fig. 4 (no pulse curve). The plasmon loss of the main peak shifts in energy from 17 to 21 eV after the first two pulses, as observed in Fig. 4. The energy shift of this plasmon loss has been shown to be characteristic of SiC.[13] The shape and intensity of the EELS curves continue changing as the num-

ber of deposition pulses is increased, as shown in Fig. 4, but no significant variation is observed beyond ten pulses of deposition. Plasmon losses in the EELS spectra of the pyrolytic graphite target and the resulting film after ten laser pulses are compared in Fig. 5. They both show a sharp peak at 28 eV and a broad peak at 55 eV, but the curve for the film shows a well defined shoulder at 6 eV loss energy, a fingerprint for well ordered graphite like HOPG.[13,15] The XPS characterization results are shown in Fig. 6. After one pulse, a sharp peak at 283.7 eV, characteristic of SiC, shifts to 285.1 eV, corresponding to the C $(1s)$ binding energy, for ten laser pulses.[13,25]

The atomic concentrations of Si and C as functions of the number of laser pulses and film thickness have been estimated from the AES and XPS spectra. The experimental data fit well to the theoretical model presented in Sec. IV, as shown in Figs. 7 and 8, for very thin carbon films. Deviations from the exponential behavior were not observed, this confirms the predicted linear relationship between d and N given by Eq. (9) and also means the carbon film is very uniform and homogeneous. However, the atomic concentration of Si and C for the same film thickness are different, as shown from Figs. 7 and 8. For instance, $X_C = X_{Si} = 0.5$ for $N \approx 2$ pulses from AES data, as observed from Fig. 7, but $X_C = X_{Si} = 0.5$ for $N \approx 11$ pulses from XPS data, as observed from Fig. 8. This is due to the fact that photoemitted electrons from the Si $(2p)$ core level, $E_{Si}(2p) \approx 1385$ eV, have a higher kinetic energy than ejected electrons from the Si-LVV Auger transition, $E_{Si}(LVV) \approx 92$ eV, for this application. As a consequence, the inelastic mean free path of electrons with energies $E_{Si}(2p)$ and $E_{Si}(LVV)$ moving into the C overlayer is $\lambda_{SC}(2p) \approx 34.7$ Å and $\lambda_{SC}(LVV) \approx 6.1$ Å, respectively. The difference in mean free paths explains why the Si signal is more persistent for photoelectrons than for Auger electrons, as observed from Figs. 7 and 8. This results in a X_{Si}/X_C ratio from XPS measurements larger than the one from AES measurements for a given d or N; i.e., AES is an analytical technique more superficial than XPS for the present study.

The existence of a SiC interface with a thickness from 2 to 4 Å, one to two monolayers, in the films is clearly demonstrated from the AES, EELS, and XPS spectra for the first two deposition pulses. This observation is also confirmed from Fig. 7 by observing a 1:1 stoichiometry of Si and C after two laser pulses. To inhibit diffusion of C into Si, the films were grown on a substrate at room temperature. Then, the interface formation was not due to this process, but solely to the chemical reaction of the highly energetic carbon species with Si atoms in the substrate. A buffer of SiC is an asset in the growth of carbon films because it would partially release internal stresses in the films. In fact, the lattice mismatches of C/SiC, 22%, and SiC/Si, 25%, are smaller than the lattice mismatch of C/Si, 52%.

The carbon species reaching the substrate and those ablated from the target are identical in an UHV environment due to their large mean free paths. The plume composition, only formed by neutrals and singly charged carbon ions, strongly depends on both laser beam wavelength and power density.[26] Although the plume composition was not able to be analyzed in this work, the predominant carbon ion species are believed to be C_2^+ and C_3^+. Murray *et al.*[27,28] found out that the species in a plume produced by a KrF excimer laser under experimental conditions similar to those used here are C_2^+ and C_3^+ with average kinetic energies of 55 and 18 eV, respectively.

In summary, this work shows the existence of the C/SiC/Si heterostructure in the deposition of laser ablated carbon species on Si (111) with a thickness of a few atomic layers. The relationship between number of laser pulses and film thickness is attained, Eq. (9). The carbon film in this application is found to be of the HOPG-type rather than DLC-type, as corroborated by the EELS spectra. The films also presented high adherence to the substrate, as no peeling was observed after detaching a scotch tape to the film. Actually, Qimin *et al.*[29] have shown that a SiC interface is a necessary step to enable the growth of DLC films. Further investigation needs to be pursued to find the conditions to grow DLC films by PLD.

ACKNOWLEDGMENTS

This work has been supported by a grant from CONACYT (México) through the research projects 4228-E and IF0076. The authors would like to thank Arturo Gamietea, Israel Gradilla, and A. Reyes-Serrato for technical assistance.

[1] J. T. Cheung and H. Sankur, CRC Crit. Rev. Solid State Mater. Sci. **15**, 63 (1988).
[2] J. T. Cheung and J. Horwitz, MRS Bull. **February**, 30 (1992).
[3] C. B. Collins and F. Davanloo, *Pulsed Laser Deposition of Thin Films*, edited by D. B. Chrisey and G. K. Hubler (Wiley, New York, 1994), Chap. 17.
[4] T. Venkatesan, *Pulsed Laser Deposition of Thin Films*, edited by D. B. Chrisey and G. K. Hubler (Wiley, New York, 1994), Chap. 12.
[5] M. Kanai, T. Kawai, and S. Kawai, Appl. Phys. Lett. **58**, 771 (1991).
[6] M. Y. Chern, A. Gupta, and B. W. Hussey, Appl. Phys. Lett. **60**, 3045 (1992).
[7] E. G. Spencer, P. H. Schmidt, D. H. Joy, and F. J. Sanasalone, Appl. Phys. Lett. **29**, 118 (1976).
[8] R. C. de Vries, Annu. Rev. Mater. Sci. **17**, 161 (1987).
[9] J. C. Angus and C. C. Hayman, Science **241**, 913 (1988).
[10] C. B. Collins, F. Davanloo, E. M. Juengerman, W. R. Osborn, and D. R. Jander, Appl. Phys. Lett. **54**, 216 (1989).
[11] D. L. Pappas, K. L. Saenger, J. Bruley, W. Krakow, J. J. Cuomo, T. Gu, and R. W. Collins, J. Appl. Phys. **71**, 5675 (1992).
[12] D. N. Belton, S. J. Harris, S. J. Schmieg, A. M. Weiner, and T. A. Perry, Appl. Phys. Lett. **54**, 416 (1989).
[13] D. N. Belton and S. J. Harris, J. Vac. Sci. Technol. A **8**, 2353 (1990).
[14] J. A. Martin, L. Vazquez, P. Bernard, F. Comin, and S. Ferrer, Appl. Phys. Lett. **57**, 1742 (1990).
[15] J. A. Martín-Gago, J. Fraxedas, S. Ferrer, and F. Comin, Surf. Sci. Lett. **260**, L17 (1992).
[16] R. J. Hamers, R. M. Tromp, and J. E. Demuth, Phys. Rev. B **34**, 5343 (1986).
[17] R. J. Hamers, U. K. Köhler, and J. E. Demuth, J. Vac. Sci. Technol. A **8**, 195 (1990).
[18] J. F. Watts, *An Introduction to Surface Analysis by Electron Spectroscopy* (Oxford University Press, Oxford, 1990), Microscopy Handbooks 22, Chap. 5.
[19] P. R. Chalker, *Diamond and Diamond-like Coatings*, edited by R. E. Clausing, L. L. Horton, J. C. Angus, and P. Koidl (Plenum, New York, 1991), NATO AST Series, p. 127.

[20]M. P. Seah, *Practical Surface Analysis, Vol 1: Auger and X-ray Photoelectron Spectroscopy*, edited by D. Briggs and M. P. Seah (Wiley, Chichester, 1990), Chap. 5.
[21]C. J. Powell, Surf. Interface Anal. **10**, 349 (1987).
[22]S. Tanuma, C. J. Powell, and D. R. Penn, Surf. Interface Anal. **17**, 917 (1991).
[23]A. Jablonski and C. J. Powell, Surf. Interface Anal. **20**, 771 (1993).
[24]T. W. Haas, J. T. Grant, and G. J. Dooley III, J. Appl. Phys. **43**, 1853 (1972).
[25]R. J. Tench, M. Baloooch, A. L. Connor, L. Bernardez, B. Olson, M. J. Allen, and W. J. Siekhaus, Mater. Res. Soc. Proc. **191**, 61 (1990).
[26]P. T. Murray, D. Thebert-Peeler, and D. V. Dempsey (1992).
[27]P. T. Murray and D. Thebert-Peeler, *Proceedings of the 2nd International Conference on Laser Ablation: Mechanisms and Applications-II, Knoxville, TN, April 1993*, edited by J. C. Miller and D. B. Geohegan (AIP Press, New York, 1993).
[28]P. T. Murray and D. T. Peeler, J. Electron. Mater. **23**, 855 (1994).
[29]W. Qimin, C. Qinggui, S. Rihua, D. Rongkang, and Z. Jian, J. Hard Mater. **6**, 45 (1995).